

Chapter 14

Synchronizations of Microseismic Oscillations as the Indicators of the Instability of a Seismically Active Region

G.A. Sobolev, A.A. Lyubushin, and N.A. Zakrzhevskaya

14.1 Introduction

Nearly all models of earthquake preparation are known to indicate magnification of the collective component in the behavior of geophysical fields in the preparation zone as the moment the earthquake occurrence is approached. The geophysical monitoring is aimed at the detection of the so-called *synchronization signal* in variations of different geophysical parameters, as well as its duration and frequency range.

It is the synchronization and collective behavior of measured characteristics that are relevant to the problems of monitoring and preparation of an earthquake or other natural catastrophes. In this respect, certain methodological recommendations can be suggested which result from the most general regularities of the system behavior; we mean the regularities that draw a system nearer to a bifurcation, or catastrophe [Nicolis, Prigogine; 1989]. An increase in the fluctuation correlation radius in the bifurcation vicinity indicates that the system tends to be self-consistent throughout its volume, thereby preparing for the collective transition to a new state. In the statistical physics of fluids, such a behavior is known as “critical opalescence” or abnormal dispersion, and is considered as a universal signal of the approaching catastrophe.

To extract hidden synchronization effects we applied the method using the estimation of canonical coherences in a moving time window developed in [Lyubushin, 1998, 2007] for the detection of earthquake precursors from geophysical monitoring data. This method was applied in [Lyubushin et al., 2003, 2004] to the analysis of multivariate hydrological and oceanographic (water-level valued) time series. The method consists in the estimation of the frequency dependent measure of the coherent behavior of components of multivariate time series, and its essentials are outlined below.

G. Sobolev (✉), A.A. Lyubushin, and N.A. Zakrzhevskaya
Schmidt Institute of Physics of the Earth, Russian Academy of Sciences, 10 Bol'shaya Gruzinskaya, Moscow, Russia
e-mail: sobolev@ifz.ru; lyubushin@yandex.ru

A complex structure of geophysical data and a high level of noises of different origin lead to the necessity of preprocessing time series and making a transition from initial data to some other parameters, which describes the most general properties of each time series. Here we take an argument providing maximum to multi-fractal singularity spectra of initial monitoring signals as such a parameter. In fractal analysis, this quantity is known as generalized Hurst exponent. The singularity spectra are estimated within moving time window of a certain length. Thus, there is a transfer from the analysis of variations of initial geophysical parameters to the analysis of generalized Hurst exponent variations. This preprocessing step turns to be rather efficient for detecting synchronization before strong earthquakes.

14.2 Initial data

We have taken broad-band vertical component seismic records with 20 Hz sampling rate from IRIS stations before 3 strong events: Kronotskii (Kamchatka Peninsula) $M = 7.7$ earthquake of December 5, 1997, [54.64°N, 162.55°E] and Hokkaido $M = 8.3$ earthquake of September 25, 2003 [41.81°N, 143.91°E]. The initial data were kindly provided by the Geophysical Service of the Russian Academy of Sciences.

For the case of Kronotskii earthquake we studied records of seismic stations in Petropavlovsk-Kamchatskii, (PET), Yuzhno-Sakhalinsk (YSS), Magadan (MAG), Yakutsk (YAK) and Obninsk (OBN), whose location is shown in Fig. 14.1.

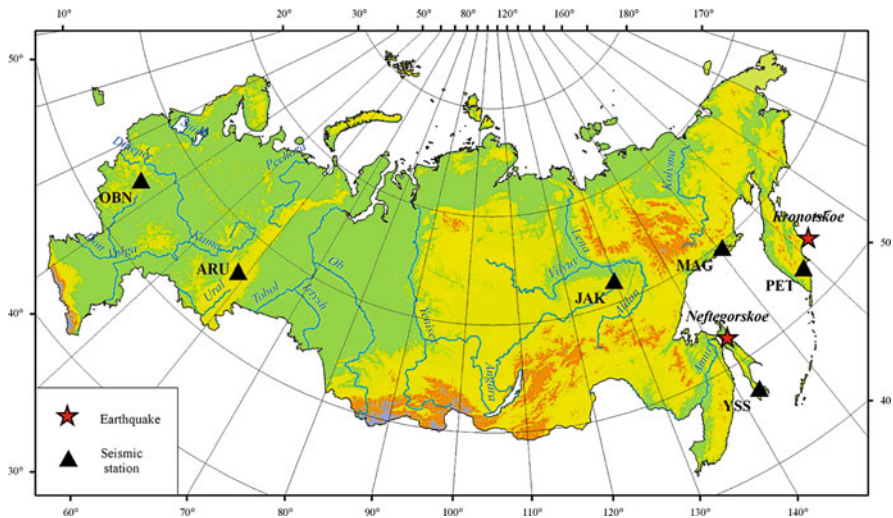


Fig. 14.1 Position of the IRIS stations whose records were analyzed before the Kronotski earthquakes. The epicenters of the earthquakes are shown by stars

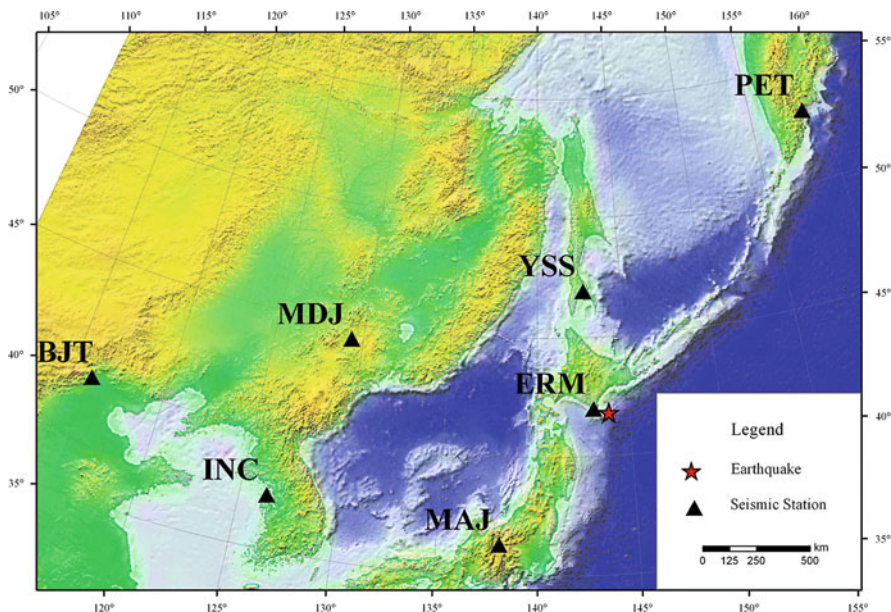


Fig. 14.2 Position of the IRIS stations whose records were analyzed before the Hokkaido earthquake. The epicenter of the earthquake is shown by star

For the case of Hokkaido earthquake we have taken data from stations ERM, MAJ, INC, MDJ, BJT, PET, YSS, which are shown in Fig. 14.2. All these stations are located at distances from 70 up to 7160 km from epicenters under different geological conditions.

The time intervals we have analyzed before earthquakes are the following:

- Kronotskii earthquake: November 05 – December 05 of 1997;
- Hokkaido earthquake: September 01 – 25 of 2003.

In previous studies [Sobolev et al., 2005; Sobolev, Lyubushin, 2006] we have found that the main precursory information is contained within low-frequency variations of microseismic background. Thus, for the transition to a minute range of periods, the initial records were averaged and downsampled 600 times, which gave time series with a sampling interval of 30 sec.

14.2.1 Brief description of the methods

14.2.1.1 Transforming to generalized Hurst exponent variations

Below we describe briefly the main points of estimating multi-fractal measure of coherence which is based on the analysis of generalized Hurst exponent

variations. More detailed description could be found in [Lyubushin, Sobolev, 2006; Lyubushin, 2007].

The analysis of fractal and multifractal properties of geophysical monitoring time series is a promising direction of data analysis in the physics of the solid Earth [Currenti et al., 2005; Telesca et al., 2005; Lyubushin, 2007]. This is due to the fact that the fractal analysis can effectively explore signals that, in terms of covariance and spectral theory, are no more than white noise or Brownian motion.

Let $X(t)$ be some signal. Let us define its variability measure $\mu(t, \delta)$ on the time interval $[t, t + \delta]$ as the range:

$$\mu(t, \delta) = \max_{t \leq s \leq t+\delta} X(s) - \min_{t \leq s \leq t+\delta} X(s). \tag{14.1}$$

A Holder-Lipschitz exponent $h(t)$ for time moment t is defined as the limit:

$$h(t) = \lim_{\delta \rightarrow 0} \frac{\ln(\mu(t, \delta))}{\ln(\delta)} \tag{14.2}$$

i.e., in the vicinity of time moment t , variability measure $\mu(t, \delta)$ tends to zero when $\delta \rightarrow 0$ according to the formula $\delta^{h(t)}$.

Singularity spectrum $F(\alpha)$ is defined [Feder, 1989] as a fractal dimensionality of the set of time moments t , for which $h(t) = \alpha$, i.e. having the same Holder-Lipschitz exponent α . Singularity spectrum exists for scale-invariant signals $X(t)$. Let us calculate a mean value of variability measure $\mu(t, \delta)$ at the power q :

$$M(\delta, q) = M\{(\mu(t, \delta))^q\}. \tag{14.3}$$

The random process $X(t)$ is scale-invariant if the value of $M(\delta, q)$ tends to zero when $\delta \rightarrow 0$ according to the formula $\delta^{\kappa(q)}$, i.e., the following limit exists:

$$\kappa(q) = \lim_{\delta \rightarrow 0} \frac{\ln M(\delta, q)}{\ln(\delta)}. \tag{14.4}$$

If the function $\kappa(q)$ is linear: $\kappa(q) = Hq$, where $H = const$, $0 < H < 1$, then the process is called mono-fractal. For Brownian motion $H=0.5$. The process $X(t)$ is called multi-fractal if function $\kappa(q)$ is nonlinear.

If the spectrum $F(\alpha)$ is estimated in a moving window, its evolution can give information on the variation in the structure of chaotic pulsations of the series. In particular, the position and width of the support of the spectrum $F(\alpha)$, i.e., the values α_{min} , α_{max} , $\Delta\alpha = \alpha_{max} - \alpha_{min}$, and $\alpha^*(F(\alpha^*) = \max_{\alpha} F(\alpha))$ are characteristics of the noise. The value α^* can be called a generalized Hurst exponent. In the case of a mono-fractal signal, the quantity $\Delta\alpha$ should vanish and $\alpha^* = H$. As regards the value of $F(\alpha^*)$, it is equal to the fractal dimension of points in the vicinity of which the scaling relation (4) holds true. Usually $F(\alpha^*) = 1$, but there exist windows for which $F(\alpha^*) < 1$.

To estimate the singularity spectrum $F(\alpha)$, we used Detrended Fluctuation Analysis (DFA) [Kantelhardt et al., 2002]. All details are described in [Lyubushin, Sobolev, 2006; Lyubushin, 2007].

14.2.1.2 Spectral measure of synchronization

Spectral measure of synchronization $\lambda(\tau, \omega)$ is defined as a product of absolute values of canonical coherences [Lyubushin, 1998, 2007]:

$$\lambda(\tau, \omega) = \prod_{j=1}^q |v_j(\tau, \omega)| \quad (14.5)$$

Here q is the dimensionality of multiple time series, ω the frequency, τ the right-hand end time coordinate of moving time window which is composed of a certain number of adjacent samples, $v_j(\tau, \omega)$ the canonical coherence of j -th scalar component which describes the strength of linear relations of this component with all other components of multiple time series. The value of $|v_j(\tau, \omega)|^2$ is a generalization of the usual squared coherence spectrum between 2 scalar time series for the case when the 2nd series is multidimensional but not scalar. The inequality $0 \leq |v_j(\tau, \omega)| \leq 1$ takes place and the closer the value of $|v_j(\tau, \omega)|$ to unity, the stronger the linear relation between variations of j -th scalar component at the frequency ω within time window with coordinate τ and analogous variations of all other scalar components. Thus, the value $0 \leq \lambda(\tau, \omega) \leq 1$ describes the effect of coherent (synchronous, collective) behavior of all scalar signals included in the considered multiple time series.

Note that, by definition, the quantity $\lambda(\tau, \omega)$ lies in the interval $[0, 1]$, and the closer its value to unity, the stronger the coherence between variations of the components of the multivariate series at the frequency ω . We should emphasize that the comparison of absolute values of the statistic $\lambda(\tau, \omega)$ is possible only for the same number q of simultaneously processed time series because, by virtue of formula (5), with increasing q , the value of $\lambda(\tau, \omega)$ decreases as the product of q values smaller than unity. If $q=2$, measure (5) is the ordinary squared modulus of the coherence spectrum.

To implement this method it is necessary to have a spectral matrix estimate within each time window. To calculate spectral matrix we used a vector autoregression model of 3rd order [Marple, 1987].

14.3 Synchronization of microseismic oscillations within minute range of periods

Figure 14.3 presents variations of generalized Hurst exponent α^* estimated within moving time windows of the 12 h length (1440 samples with 30 s time interval) taken with mutual shift of 1 h (120 samples) for 5 seismic stations with positions

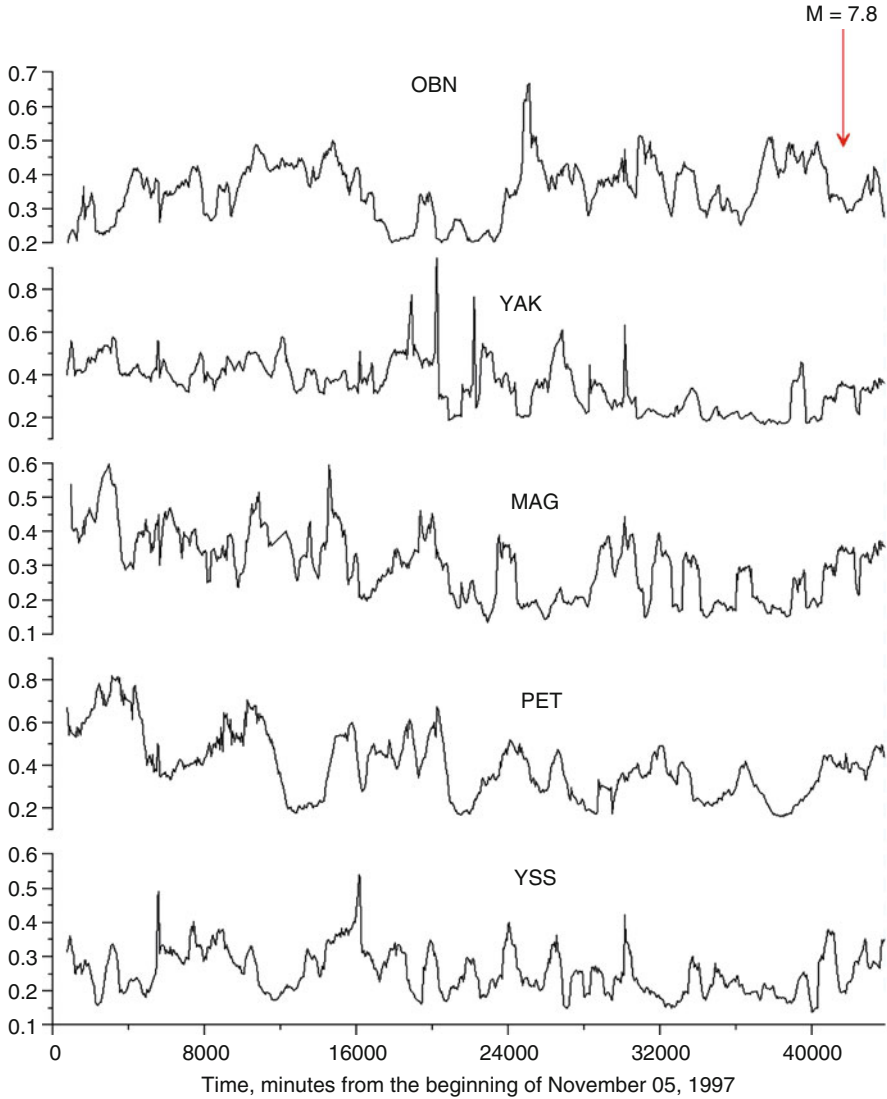


Fig. 14.3 Before the Kronotskii earthquake. Plots of the generalized Hurst exponent α^* realizing the maximum of the singularity spectrum of the micro-seismic background at all stations with the estimation in a moving 12 h wide time window with a shift of 1 h. The coordinate of the right-hand end of the moving time window is plotted on the time axis

presented in Fig. 14.1. Scale-dependent trends following from tidal and temperature influences in DFA-technique were removed by local polynomials of 4th order. We have taken an interval of 30 days length before the Kronotskii earthquake. A further analysis provides estimation of spectral measure of synchronization (5) for time series of α^* -variations (Fig. 14.3). The length of moving time window for obtaining

statistics $\lambda(\tau, \omega)$ was taken to be 109 samples. Because each α^* -value is obtained from time window of 12 h length with a shift of 1 h, this means that the length of time window for the measure (5) is $(109-1) \cdot 1 + 12 = 120 \text{ h} = 5 \text{ days}$.

Figure 14.4 presents time-frequency diagrams of statistics (5) for different combinations of stations. A main burst of coherence is concentrated within range of time marks 40000-42000 minutes, i.e., a few days before the earthquake. In the process of approaching of moving time window to the moment of the main shock the α^* -variations coherence decreased although still remained at the level which is

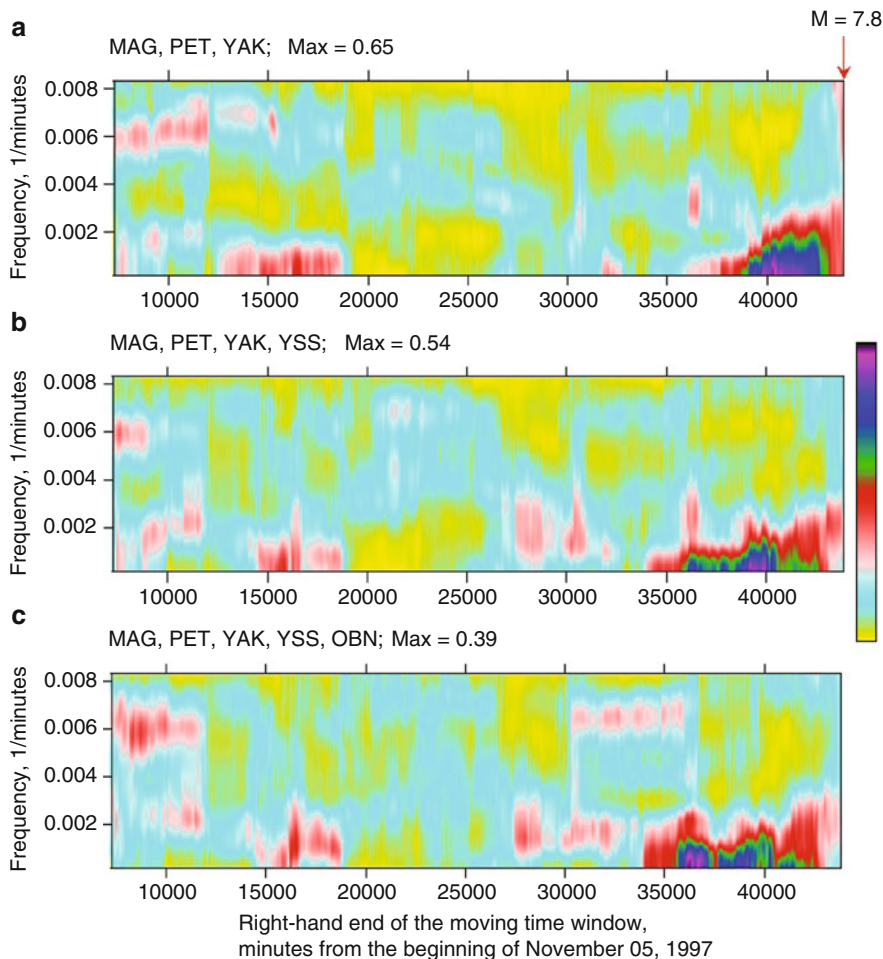


Fig. 14.4 Before the Kronotskii earthquake. Frequency–time diagrams of the evolution of the spectral measure of coherence of α^* variation spectral series with the estimation in the moving time window 109 samples (5 days) long for a successively increasing number of simultaneously analyzed stations. Maximum values of the coherence measure are shown in each diagram after the codes of the stations analyzed

higher than the background of statistical fluctuations. Time-frequency diagrams in Fig. 14.4 testify that the length of time span of “coherence spot” increases with increasing number of analyzed stations.

Series of diagrams $\lambda(\tau, \omega)$ were calculated to check the stability of the low frequency coherence pulsation in the vicinity of the time mark 40000 min by estimating the results of various combinations of three stations. Note that it is admissible to compare maximum values of the coherence measure because the number of simultaneously analyzed time series is the same. The highest peak of coherence (0.65) is observed for the MAG, PET, and YAK stations, at Kronotskii earthquake epicentral distances of 900, 350, and 2050 km, respectively; the peak is the lowest (0.32) for the OBN, ARU, and YAK stations, which are the farthest from the earthquake source (6800, 5900, and 2050 km, respectively). In all variants, the coherence measure experiences a pulsation in the neighborhood of the time mark 40000 corresponding to the observation interval November 29–December 3, 1997, i. e., three to seven days before the shock.

During data analysis before the Hokkaido earthquake, seismic records of stations ERM and MAJ were not used because ERM was not working the last 4 days before the shock, whereas MAJ was not working 7 days during time interval 2 weeks before the event. A similar analysis (with the same parameters as for Kronotskii earthquake data processing) combining multi-fractal singularity spectra estimates within moving time window of 12 h length with further application of spectral measure of synchronization to α^* -variations was applied. The main result of this analysis is

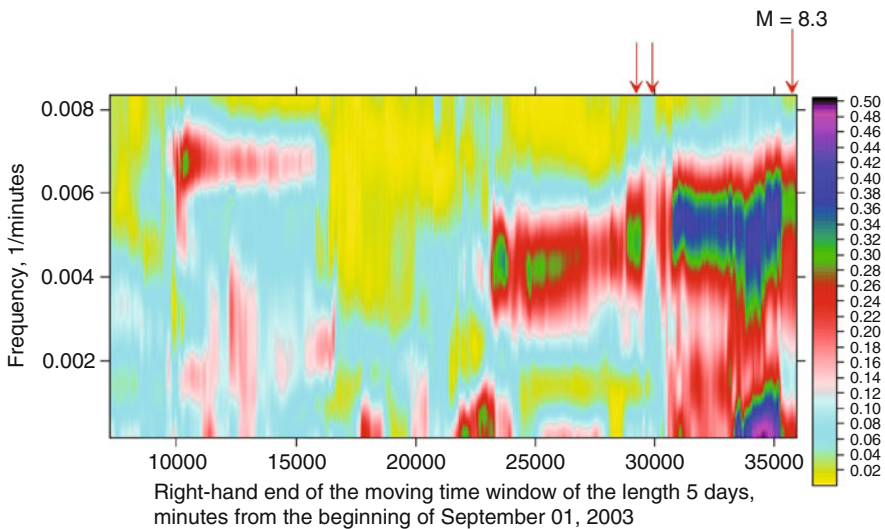


Fig. 14.5 Before the Hokkaido earthquake. Frequency–time diagrams of the evolution of the spectral measure of coherence of α^* variation spectral series with the estimation in the moving time window 109 samples (5 days) long for seismic stations YSS, MDJ, INC. Arrows indicate successive time moments of 2 remote earthquakes ($M=6.6$) and of Hokkaido earthquake (the last one)

that synchronization occurred 2 days before the Hokkaido event (interval 33000-35000 minutes from beginning of September 01, 2003). This synchronization covers range of periods from 3 h on. When different variants of 3 stations were tested, the strongest effect was observed for stations which are closest to the epicenter of future shock. Time-frequency diagram, $\lambda(\tau, \omega)$, for these stations (YSS, MDJ, INC) is presented in Fig. 14.5. The following 3 peculiarities of this diagram should be underlined: (1) synchronization at 3 h period (frequency $\sim 0.005 \text{ min}^{-1}$) began 9 days before the event (time mark 23000 minutes); (2) the brightest synchronization within wide range of periods began 2 days before the shock (time marks 33000-35000 minutes); (3) the gap in synchronization scenario within interval 29000-31000 minutes of time marks is connected with 2 remote strong earthquakes (indicated by red arrows) with magnitude 6.6. The first one has epicenter [19.72°N, 95.46°E] and occurred on September 21 and the second one has epicenter [21.16°N, 71.67°W] and occurred 10 hours later, on September 22. The arrival of seismic waves from these earthquakes with different onset times to the analyzed stations disturbed the synchronization pattern.

14.4 Conclusion

Estimates of spectral measure for variations of either low-frequency (in minute range of periods) micro-seismic background oscillations or their generalized Hurst exponents detect synchronization effect on large areas, 2-5 days before strong earthquakes. This coherence effects between different stations manifest themselves on periods: for Kronotskii earthquakes – more than 6 hours, for Hokkaido – more than 3 hours, for Sumatra earthquake – within range 2-60 minutes. The coherence measure is increasing when it is calculated for the set of stations which are closer to the epicenter of future event.

References

- Currenti G., C. del Negro, V. Lapenna, and L. Telesca (2005) Multifractality in local geomagnetic field at Etna volcano, Sicily (southern Italy) – *Natural Hazards and Earth System Sciences*, 5, 555–559, 2005
- Feder J. (1989) *Fractals*. Plenum Press, New York, London
- Kantelhardt J. W., Zschiegner S. A., Konschenly-Bunde E., Havlin S., Bunde A., and Stanley H. E. (2002) Multifractal detrended fluctuation analysis of nonstationary time series, *Physica A*, 316, 87–114, 2002.
- Lyubushin A.A. (1998) Analysis of Canonical Coherences in the Problems of Geophysical Monitoring – *Izvestiya, Physics of the Solid Earth*, vol. 34, 1998, pp. 52-58. http://alexeylyubushin.narod/Canonical_Coherences_in_the_Problems_of_Geophysical_Monitoring.pdf
- Lyubushin A.A., Pisarenko V.F., Bolgov M.V. and Rukavishnikova T.A. (2003) Study of General Effects of Rivers Runoff Variations – *Russian Meteorology and Hydrology*, 2003, No.7, pp. 59-68. http://alexeylyubushin.narod/Coherence_measures_of_rivers_runoff_time_series.pdf

- Lyubushin A.A., Pisarenko V.F., Bolgov M.V., Rodkin M.V., and Rukavishnikova T.A. (2004) Synchronous Variations in the Caspian Sea Level from Coastal Observations in 1977–1991. – Atmospheric and Oceanic Physics, 2004, Vol. 40, No.6, pp. 737-746. http://alexeylyubushin.narod/Canonical_Coherences_of_Caspian_Sea_Level_Variations.pdf
- Lyubushin A.A. and G.A. Sobolev (2006) Multifractal Measures of Synchronization of Microseismic Oscillations in a Minute Range of Periods – Izvestiya, Physics of the Solid Earth, vol.42, No.9, 2006, pp.734-744. http://alexeylyubushin.narod/Multifractal_Measures_of_Synchronization_of_Microseismic_Oscillations.pdf
- Lyubushin A.A. (2007) Geophysical and ecological monitoring systems data analysis. Moscow, 'Nauka', 228 p. (in Russian). http://alexeylyubushin.narod/Geophysical_Monitoring_Systems_Data_Analysis_Book_Rus.pdf
- Lyubushin A.A. and G.A. Sobolev (2007) Synchronization effects of microseismic background oscillations field before strong earthquakes – IUGG XXIV General Assembly “Earth: our changing planet”, Perugia, Italy, July 02–13, 2007. Session SS005 “Earthquake Sources – Modeling and Prediction”.
- Marple S.L. (Jr.) (1987) Digital spectral analysis with applications. Prentice-Hall, Inc., Englewood Cliffs, New Jersey.
- Nicolis G. and I. Prigogine (1989) Exploring Complexity. An introduction. W.H.Freeman and Company. New York, 1989.
- Sobolev G.A. (2003) Evolution of Periodic Variations in the Seismic Intensity before Strong Earthquakes – Izvestiya, Phys. Solid Earth, 2003, vol.39, No.11, 2003, pp. 873–884.
- Sobolev G.A. and A.A. Lyubushin (2006) Microseismic Impulses as Earthquake Precursors – Izvestiya, Physics of the Solid Earth, vol. 42, No.9, 2006, pp.721-733.
- Sobolev G. A. and A. A. Lyubushin, “Microseismic Anomalies before the Sumatra Earthquake of December 26, 2004,” Fiz. Zemli, No. 5, 3–16 (2007) [Izvestiya, Phys. Solid Earth 43, 341–353 (2007)].
- Sobolev G. A., A. A. Lyubushin, and N. A. Zakrzhevskaya, “Asymmetric Impulses, Periodicities and Synchronization of Low-Frequency Microseisms,” Vulkanol. Seismol., No. 2, 135–152 (2008).
- Sobolev G.A. and A.A. Lyubushin (2007) Using Modern Seismological Data for Earthquake Precursors Detecting – Russian Journal of Earth Sciences, in press.
- Telesca L., G. Colangelo, and V. Lapenna (2005) Multifractal variability in geoelectrical signals and correlations with seismicity: a study case in southern Italy – Natural Hazards and Earth System Sciences, 5, 673–677, 2005.